At-Wavelength Metrologies for Extreme Ultraviolet Lithography

D. ATTWOOD*, E. ANDERSON, P. BATSON, R. BEGUIRISTAIN*, J. BOKOR*, K. GOLDBERG*, E. GULLIKSON, K. JACKSON, K. NGUYEN**, M. KOIKE, H. MEDECKI, S. MROWKA, R. TACKABERRY, E. TEJNIL* and J. UNDERWOOD

*Lawrence Berkeley National Laboratory, *Also University of California, Berkeley, **Now at Advanced Micro Devices (AMD)*

1. Introduction

The manufacturing of electronic devices with ever smaller feature sizes provides a continuing challenge to the technological community[1]. At present, manufacturing is in a transition from electronic structures with 0.35 μm critical dimensions to structures with 0.25 μm critical dimensions. To provide the necessary resolution improvement, optical lithography tools used to define the circuit patterns are in progression from using 365 nm wavelength light from a mercury discharge lamp to using 248 nm ultraviolet radiation from a krypton fluoride (KrF) laser. Further progressions to 0.18 and 0.13 μm critical dimension are anticipated with argon fluoride (ArF) lasers at 193 nm, following as close as possible an evolutionary path that minimizes the introduction of new technologies wherever possible, but also by its very nature and goals constantly introduces new capabilities and techniques. At 0.13 μm and beyond some expect that substantially new technologies may be introduced, including x-ray proximity or electron beam techniques[1]. An alternate approach, based on the use of extreme ultraviolet radiation with wavelengths in the region of 10-14 nm, follows a path closer to evolutionary progression, with possible market entry at 0.13 or 0.1 μm and a lifetime of several generations. This approach is based on a transition to reflective optics with numerical aperture near 0.1 and a substantial decrease in wavelength, by a factor of about fifteen. Thus while continuing to follow a path involving projection optics, extreme ultraviolet lithography (EUVL) proposes a dramatic reduction in wavelength. This has the great advantage of permitting the writing of patterns with ever smaller feature sizes. In addition, use of a lower numerical aperture provides a sufficient depth of focus, which is of great interest to the manufacturing community.

The general idea of extreme ultraviolet (EUV) lithography[2,3] is shown schematically in ***Fig 1.*** All reflective optics produce an image of a reflective mask with a top surface absorber pattern, with nominally five to one reduction, printing patterns to 0.1 μm feature size over a several square centimeter wafer area. Most critical to EUVL is the enabling technology of high reflectivity coatings[4], in this case resonant interference coatings, commonly referred to as multilayer (ML) coatings in the EUV and soft x-ray communities[5], but more familiar to some as extensions of quarter wave ($\lambda/4$) stacks for visible light. Because of substantial absorption of radiation by all materials at EUV wavelengths[6], the engineering of these optical coatings requires significant innovation. Furthermore, the individual layers are $\lambda/4$ in thickness (about 3 nm at EUV wavelengths), so that interface roughness, interdiffusion, and thermal and mechanical stability provide substantial challenges to the optical coating and materials science communities[7,8]. Nonetheless, normal incidence reflectivities of 65 to 70%, or nearly the theoretical maxi-

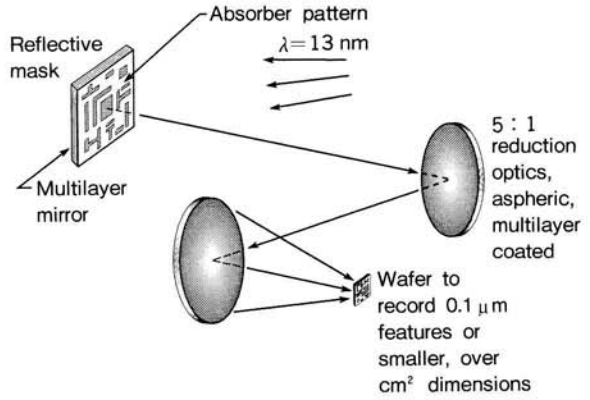

Fig. 1 **Extreme ultraviolet (EUV) lithography is illustrated schematically, showing multilayer coated reflective optics used to image a mask pattern at a nominal 5 : 1 reduction at the wafer.** With nominally 11–14 nm wavelength, features of order 100 nm can be printed with relatively low numerical aperture, thus providing significant depth of focus.

mum, have been obtained[9].

A second major challenge is the fabrication of diffraction limited, large-field optics[10]. Because of finite reflectivity, the optical systems necessarily utilize a minimal number of mirrors and require aspherical mirror surfaces. This provides particular challenges as fabrication must be accomplished with attention to surface figure and roughness, including the control of intermediate spatial frequencies, which collectively affect resolution, throughput, and contrast[11]. Substantial progress has been made in the fabrication of aspheric optics for EUV wavelengths[12-14]. As the coatings follow a Bragg relationship with regard to wavelength, d-spacing, and angle of incidence, it is important to employ optical designs that minimize required variations in d-spacing and to carefully engineer d-spacing variation control[15-17]. Further attention must be paid to such issues as stress[18] and surface contamination[19].

For the success of a new lithography program it is essential that the appropriate infrastructure exist; in particular, the metrologies that are required to evaluate progress towards specific technical goals and milestones. With the emphasis on 0.1 μm resolution, wide-field, aspheric optics, it is critical that there be an appropriate extension of visible light interferometry for in-shop substrate inspection[20]. As EUV lithography employs resonant multilayer interference coatings, it is also critical a full set of "at-wavelength" metrological tools be available for the characterization of coatings, optical components and optical systems. For example the multilayer coatings will typically require that d-spacings be held to 1% tolerances across the individual optics[5-17]. From small deviations in the prescribed d-spacing values, significant phase errors in the reflected wavefront are quickly accumulated, as illustrated[16] in ***Fig. 2***. As the effective d-spacing is dependent on material refractive indices, which will vary with localized material structure due to crystallization, diffusion and heating, it is essential that appropriate d-spacing measurements be made at the wavelength of ultimate use. Furthermore, to assess wavefront errors after coating and mounting, it is also essential that an "at-wavelength" interferometer be available for final system positioning and alignment, with a wavefront accuracy of better than $\lambda_{EUV}/30$. In the following sections we discuss challenges and progress in the development of at-wavelength measurements of multilayer reflectivity and scattering, at-wavelength interferometry, and at-wavelength mask defect inspection.

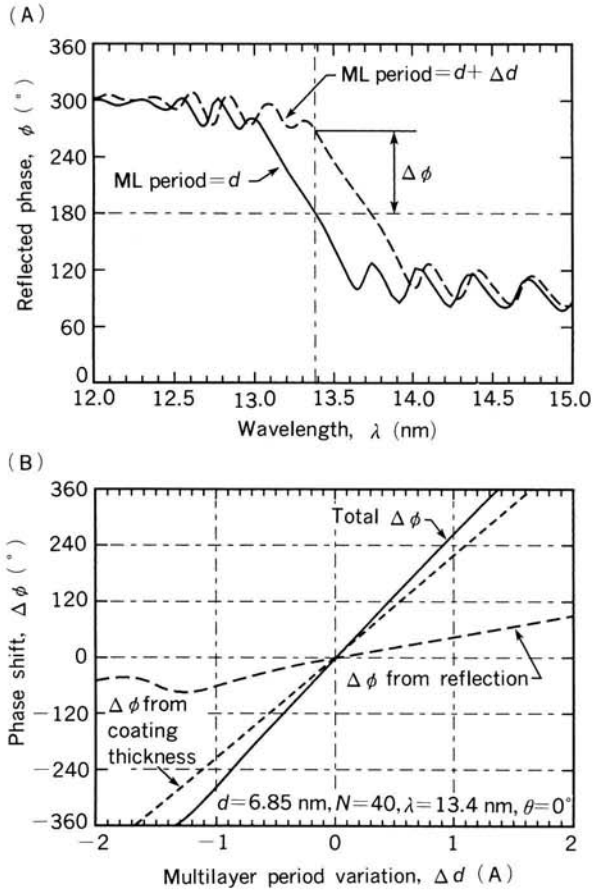

Fig. 2 **(A) Phase shift on reflection for two Mo/Si ML coatings near normal incidence, whose periods differ by an amount Δd. (B) Phase error introduced by a ML coating; due to variation in phase shift on reflection (dashed); due to phase shift resulting from optical path difference corresponding to total coating thickness (dotted); and total phase shift (solid).** From D.L. Windt *et al.*, Ref. 16.

2. Reflectivity

The key technology enabling the development of EUV lithography is the ability to make high-reflectivity mirrors[4,9]. A side-view TEM image of a molybdenum/silicon multilayer mirror is shown in ***Fig. 3***. ***Figure 4*** and ***Fig. 5***

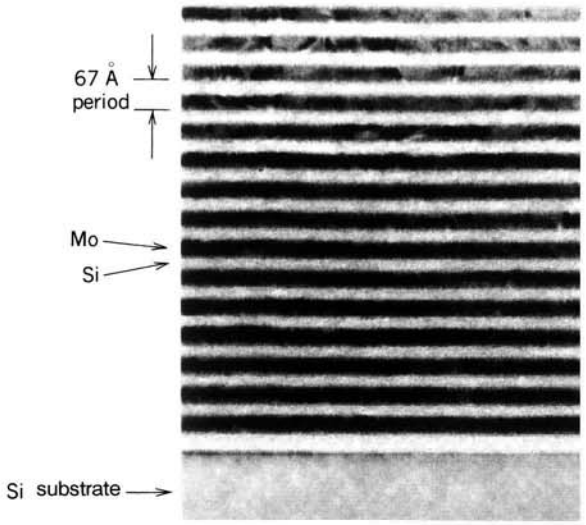

Fig. 3 **A transmission electron micrograph of a 6.7 nm period molybdenum/silicon mirror** (courtesy of Dr. T. Nguyen, formerly of CXRO/LBNL, now at Lawrence Livermore National Laboratory).

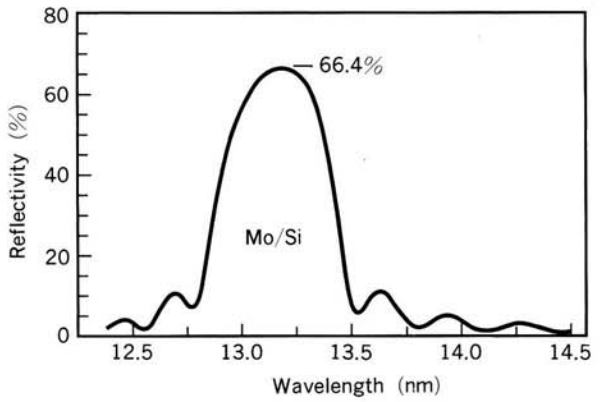

Fig. 4 **Measured reflectivity curve for a molybdenum/silicon multilayer mirror** (Ref. 21).

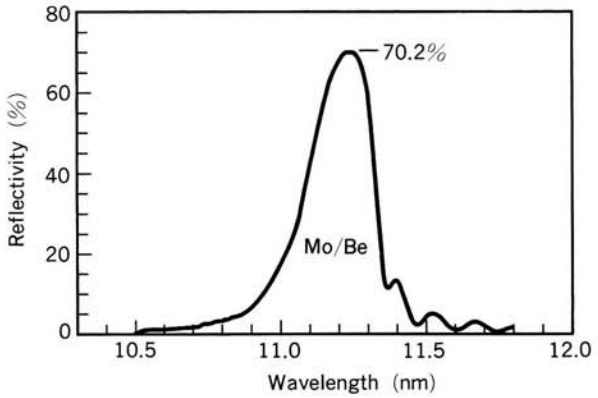

Fig. 5 **Measured reflectivity curve for a molybdenum/beryllium multilayer mirror** (Ref. 9).

show measured reflectivity curves as a function of wavelength for Mo/Si and Mo/Be multilayer mirrors, respectively. The much studied Mo/Si systems achieve a reflectivity of 66.4% in the example shown[21]. The Mo/Be mirror achieved a peak reflectivity of 70.2% in early experiments[9]. Both mirrors were measured at the new EUV Calibrations and Standards beamline[22] at Lawrence Berkeley National Laboratory (LBNL). The precision metrology beamline, which covers a spectral region from 50 to 1,000 eV (1-25 nm wavelength), is shown schematically in ***Fig. 6***. The beamline employs a varied line space grating[23] monochromator and a novel order-sorting mechanism. It provides a photon flux of 10^{12} ph/sec in a relative spectral bandwidth of 10^{-3}, with high spectral purity. Beamline optics permit the radiation to be focused to a 10-50 μm spot size on the mirror being studied. By the mechanical nature of its design the system is inherently wavelength self-calibrated. Standard emission lines and absorption edges are measured to an accuracy of 1/7000. Reflectance is nominally measured to 0.1% accuracy. The reflectometry chamber is shown in ***Fig. 7***. The chamber accepts optics up to 250 mm diameter. With precision rectilinear and angular motions of the optics and various apertures, the facility can be used to accurately map reflectivity as a function of position and angle across the optic under test. Because of its flexibility, the facility is also used to study EUV scattering, refractive index and spatially resolved materials properties (micro-ESCA)[24].

An issue of particular significance for the success of EUV lithography is the control of phase variations across the wavefront as it propagates and reflects through the imaging optical system. Windt[16] has calculated the phase shift due to variations in multilayer d-spacings, showing substantial phase shifts due to both the resonant nature of reflection from a multilayer interference structure as well as from the geometrical movement of the front surface. It is clear from these studies (see ***Fig. 2***) that d-spacings must

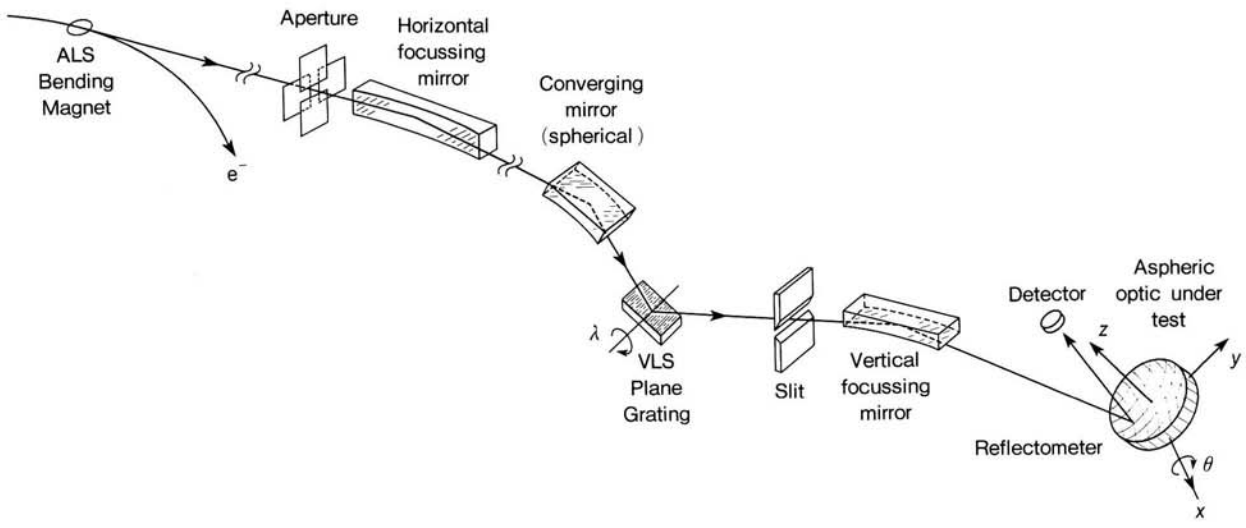

Fig. 6 **A beamline specially built for high accuracy measurements at EUV wavelengths.** Beamline was built and is operated by LBNL's Center for X-ray Optics.

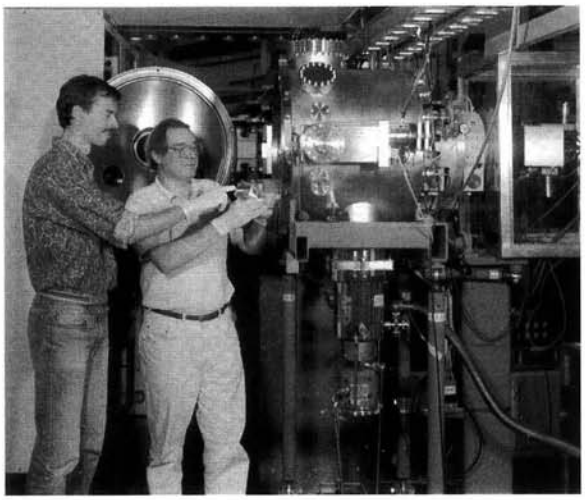

Fig. 7 **The EUV reflectometry and scattering chamber for testing coated optics.** Shown are Drs. E. Gullikson (l.) and J. Underwood (r.).

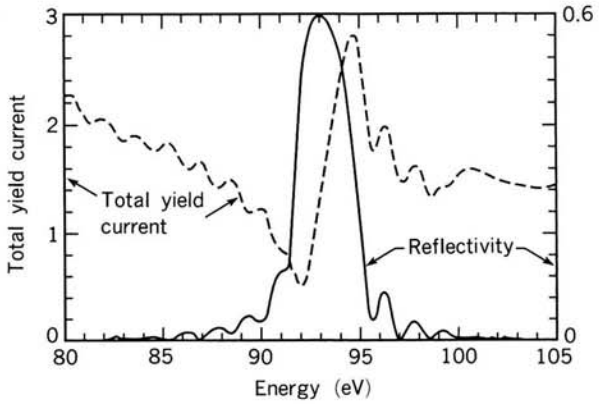

Fig. 8 **Reflectivity and photoelectric current are measured as photon energy is tuned through the Bragg peak, revealing the phase of standing waves within the multilayer structure** (from J.H. Underwood, Ref. 25).

be maintained to departures from specifications of 1% or less across each surface. A measurement of phase effects[25] in multilayer mirrors is shown in ***Fig. 8***, where we see both at-wavelength reflectivity and total photoelectric yield from the surface as photon energy is scanned using the beamline shown previously in ***Fig. 6***. The variation of current results from the location of the standing wave within the multilayer, and particularly at the surface, as wavelength is tuned through the Bragg peak. The phase variation is seen to be approximately π radians as the wavelength is tuned through the full-width of the central reflectivity lobe[25].

Thus, this high-precision tool is capable of studying wavelength resonant structures, with concomitant opportunities for critical at-wavelength metrologies.

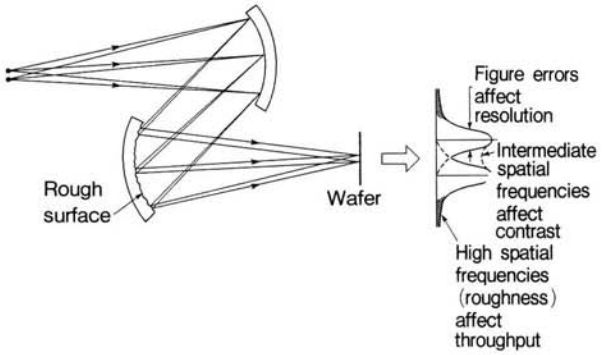

Fig. 9 **The effect of figure errors, roughness of intermediate spatial frequency, and nanoroughness, on the spatial resolution, contrast and throughput, respectively, of an optical system are illustrated.**

3. Scattering

To achieve high spatial resolution, maximum contrast, and high throughput, it is essential that an optical surface meet demanding specifications, typically to a small fraction of a wavelength, not only for surface figure[10], but also surface roughness[7,8] and intermediate spatial frequencies [11,26]. ***Figure 9*** shows two mirrors used to form an image of two closely spaced lines or points. The second optic has a non-ideal surface, with departures due to roughness and figure errors containing a very broad range of spatial frequencies. Figure errors are the lowest possible spatial frequencies, from as large as the optical diameter to some fraction thereof. Beyond the diffraction limit set by the wavelength and numerical aperture, surface errors cause a broadening of the point response function so that there is some loss of spatial resolution in the imaging system. Somewhat higher spatial frequencies (shorter scale lengths), often referred to as "intermediate spatial frequencies", provide a spray of radiation across the image plane resulting in a loss of contrast, most noticeable in the vicinity of features that are just barely resolved. Still higher spatial frequencies, with scale sizes approaching the radiation wavelength, are referred to as "nanoroughness", These very high spatial frequencies scatter radiation to large angles, removing most of the radiation from the imaging process, perhaps causing some loss of contrast, but largely lowering the optical throughput by reducing the photon flux available to expose the recording wafer[7]. These effects are illustrated in ***Fig. 9***. The two peaks are broadened by small angle scattering, which fills the otherwise dark region between them, and by the larger angle scattering from the nanoroughness, which creates the large tails.

To quantify these effects for EUV optical systems, the beamline described in ***Fig. 6*** has been carefully apertured to permit at-wavelength scattering measurements over nine orders of magnitude, at angles from less than 0.1 degrees to greater than 10 degrees. ***Figure 10*** shows an example of non-specular scattered radiation, at 13.2 nm wavelength,

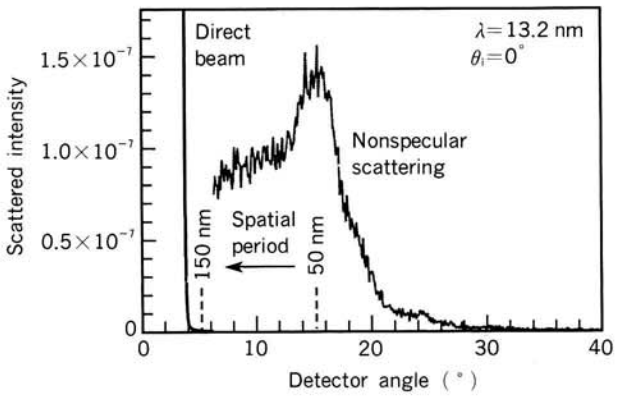

Fig. 10 **Non-specular scattering from a multilayer coated mirror removed radiation from the "reflected" beam and thus lowers reflectivity and reduces optical throughput** (courtesy of E. Gullikson, D. Stearns *et al.*, Ref. 27).

from a multilayer mirror[27]. Note that in the example cited in ***Fig. 10*** the scattering angles correspond to spatial roughness scales (wavelengths) in the region from 50 to 150 nm. Such measurements can be used to model interface roughness in multilayer mirrors[8], and thus to assess their impact on the pattern transfer process. This also provides an important at-wavelength metrological tool for assessing surface finish and multilayer coating interface definition of EUV optical components.

4. EUV Interferometry

The use of optical systems to print smaller features over larger areas will require improvements in the fabrication and polishing of optics. Improvements in optics require advances in optical metrologies. The primary tool for measuring optical surface figure is interferometry, which compares a wavefront transmitted or reflected by an optic with a reference wavefront[28,29]. Ideal spherical reference waves are spatially coherent, that is characterized by uniform phase across the wavefront, at least to the degree required for a given application. Thus the measured variations of the resultant interference ("fringe") pattern are due solely to the optic under test, and therefore can be used to deduce its imperfections or departures from specification. The metric for these measurements is the wavelength used for the evaluation of the optic.

To be sure, all advances in optical lithography towards finer critical dimension will benefit from advances in interferometry. For EUV lithography this will require advances on two fronts. For the "in-shop" measurement of optical substrates visible-light interferometry is convenient and indispensable. Towards that end significant progress has recently been reported on the development of visible-light interferometry based on the far-field diffraction from the polished end of a single-mode fiber to suitable numerical aperture[30]. With an ultimate goal of achieving an accuracy of 0.1 nm rms ($\lambda_{visible}/6000$), for the anticipated specification of 0.25 nm rms (root mean square) surface figure errors on aspheric mirrors, an accuracy of 0.5 nm rms has been reported, and several clear paths towards improvement have been identified[30].

Optical systems for EUV lithography will also require the development of "at-wavelength" interferometry as the individual optics are coated with phase-sensitive interference coatings, as was illustrated in ***Fig. 2***. It is therefore essential that final system mounting and alignment be qualified for minimal rms wavefront error with accurate at-wavelength interferometrys[31]. Towards this end, substantial progress has been reported on the development of an EUV phase-shifting point-diffraction interferometer[32,33] (PS/PDI), designed to achieve a goal of $\lambda_{EUV}/100$ rms accuracy for tunable wavelengths in the 10–14 nm range. This interferometer may also prove useful at visible and ultraviolet wavelengths[32].

The most recent version of this interferometer is shown in ***Fig. 11***. The interferometer utilizes partially coherent radiation from an undulator[34], described in the next section but not shown in ***Fig. 11***. In the object plane of the test optic, the beam is filtered by a pinhole that is small enough to coherently illuminate the optical system with an EUV wavefront of the desired uniformity. The wavefront quality is related to the entrance numerical aperture of the optic and to the quality of pinhole available[35]. The optical system brings the incident wavefront to focus in the plane conjugate to the entrance pinhole plane[28]. To measure the wavefront variations due to optical imperfections, a "reference wavefront" is required. In the version of the PS/PDI shown in ***Fig. 11***, the reference wavefront is produced through the use of a coarse diffraction grating between the entrance pinhole and optical system under test[32,33]. Although the grating generates many orders, only two are selected for propagation through to the CCD camera, which is a back-thinned electronic array detector directly sensitive to EUV light. The selection of just two orders is accomplished through the use of a focal plane mask, as shown in ***Fig. 11***, which blocks all but the zeroth (0th) order and one of the first (1st) orders of the grating. Both contain information regarding the optical system under test. To produce the reference wavefront, the first-order is spatially filtered with a very small pinhole, of order 50 nm diameter[35], in the focal plane mask. The zeroth-order wavefront, which contains the aberrations in the optical system, passes through a larger, non-filtering aperture in

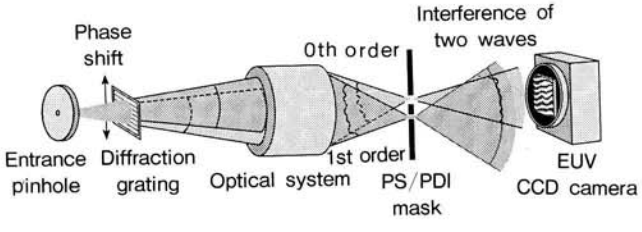

Fig. 11 **A phase-shifting point diffraction interferometer for use at EUV wavelengths.**

the focal plane mask. Considerable attention must be paid to the quality of the reference wavefront. Its dependence on pinhole symmetry and on the desired numerical aperture of the measurement sets the ultimate wavefront measuring accuracy of the interferometer.

The test and reference wavefronts overlap at the surface of the CCD camera where their mutual interference is recorded. Recording multiple fringe patterns as the diffraction grating is translated in a direction orthogonal to its lines enables the use of "phase-shifting" interferometry, permitting an accurate determination of the encoded wavefront.

The PS/PDI overcomes the shortcomings of the conventional point-diffraction interferometer (PDI)[36] by providing an intense reference wave which can undergo substantial spatial filtering and still provide sufficient photon flux to provide high-contrast fringes when mixed with the unfiltered test wavefront. Furthermore, the small reference pinhole is centered on the reference-wave focal pattern to minimize variations in the pinhole illumination. Thus the new PS/PDI is significantly more efficient with regard to throughput, provides better control over generation of the reference wave, and possesses a convenient geometry with two separate waves for testing wavefront measurement accuracy, in addition to having phase-shifting capability described above.

Tests of a multilayer-coated reflective optical system using the EUV PS/PDI are presently under with very encouraging early results. Sample fringe patterns, obtained when testing annular zone plate lenses at 13 nm with an earlier version of the interferometer, the PDI, are shown in ***Fig. 12***. Analyses of that work led to the invention[32] of the present PS/PDI described in ***Fig. 11***. An analysis[33] of a zone plate fringe pattern similar to those seen in ***Fig. 12*** is shown in ***Fig. 13***. Assuming a perfect

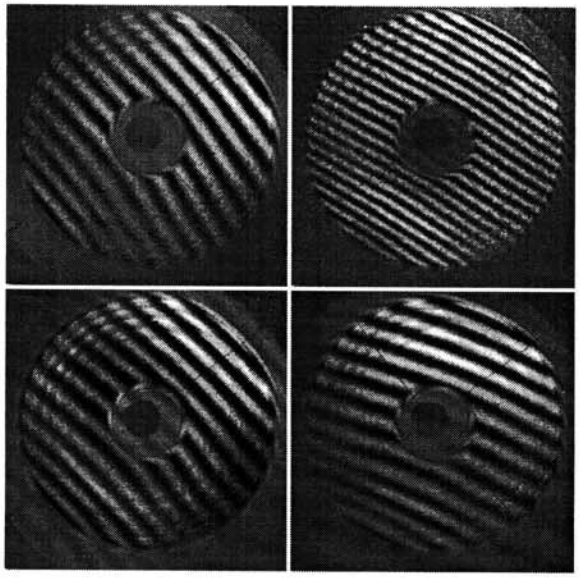

Fig. 12 **EUV fringe patterns of a zone plate lens tested with an earlier version of the PDI.**

Fig. 13 **Wavefront variations measured for an annular zone plate lens at 13 nm wavelength using an earlier version of the PDI.** The dominant aberration is 0.26 waves of astigmatism, some of which may be associated with an overly large reference pinhole used at that time (from Ref. 33).

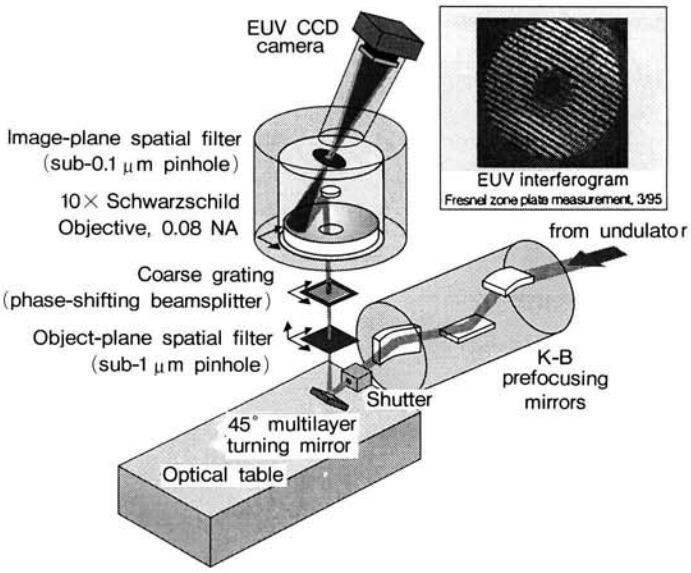

Fig. 14 **At-wavelength interferometry of a 10× Schwarzschild optic multilayer coated for 13.4 nm wavelength is presently underway using spatially coherent undulator radiation and a phase-shifting point diffraction interferometry.**

reference wavefront, this analysis indicates a dominant 0.26 waves (EUV) of astigmatism, 0.12 waves of coma, and 0.06 waves of spherical aberration. Those early measurements, however, were likely affected by use of overly large reference pinholes[33].

The present setup for EUV PS/PDI of a 10× Schwarzschild optic coated[16] for 13.4 nm wavelength is shown in ***Fig. 14***. EUV radiation from the undulator enters from the right, is deflected vertically by a multilayer-coated flat mirror where it illuminates the entrance ("object plane") pinhole, presently 0.9 μm diameter. A spatially coherent power (see next section) of about 7 μW then illuminates the grating, which serves as a phase-shifting beamsplitter. The various orders illuminate the optic under test. In the focal ("image") plane an order sorting mask selects the

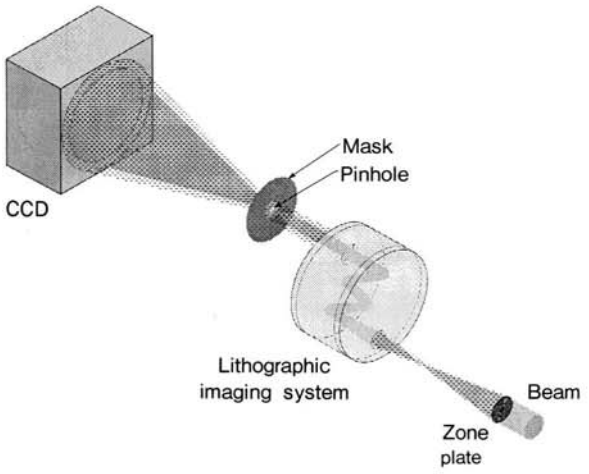

Fig. 15 **At-wavelength interferometry of an EUV lithographic optical imaging system is suggested.** The goal of this program is to achieve a wavefront measuring accuracy of $\lambda_{EUV}/100$.

two orders, which propagate to the EUV CCD recording camera. Of the two orders transmitted by the mask, the first order is spatially filtered by a nominally 50 nm pinhole, as described earlier. Experiments now underway indicate that this program is making very good progress towards a measurement accuracy of $\lambda_{EUV}/100$ for reflective optical systems. ***Figure 15*** shows schematically at-wavelength interferometry of an EUV lithographic imaging system, in which the final lens mounting and alignment will be accomplished by minimization of rms wavefront distortion.

5. Coherent EUV Radiation for Optical Testing

In the previous section it was pointed out that high accuracy $\lambda_{EUV}/100$ interferometry is best accomplished through the use of high average power, spatially coherent radiation tuned to the wavelength of choice. With presently available technologies this is best obtained through the use of undulator radiation from a small phase-space (size-angle product), relativistic electron beam traversing a periodic magnet structure[31,34]. A system specifically optimized for at-wavelength interferometry of EUV optics is illustrated in ***Fig. 16***. An 8.0 cm period magnet structure ("undulator") of 55 periods is used at LBNL's Advanced Light Source (ALS), operating at energies of 1.5 or 1.9 GeV. ***Figure 16A*** shows the undulator and pinhole-angular aperture spatial filter. ***Figure 16B*** shows the broad tunability of central cone power (containing a $1/N$ relative spectral bandwidth), typically of order one Watt into a 75 μrad half-angle cone at the ALS. After spatial filtering ***Fig. 16C***, but without further monochromatization, spatially coherent power is broadly available at an average power of order 10 mW over photon energies from

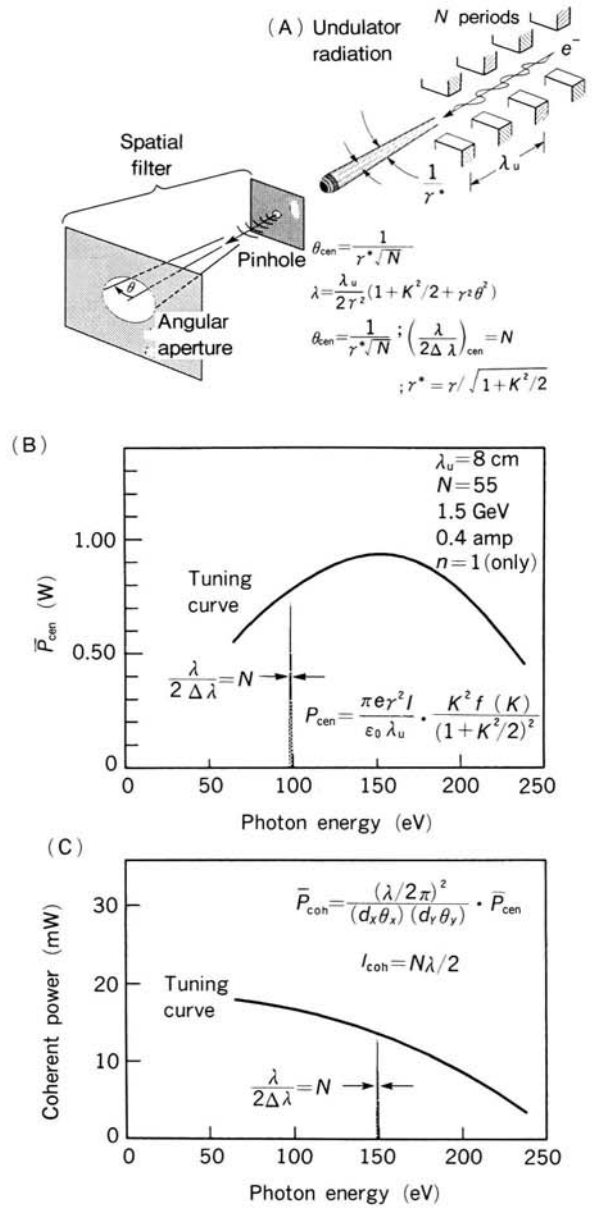

Fig. 16 **Undulator radiation at EUV wavelengths is generated by 1.5 GeV electrons traversing an 8.0 cm period magnet structure.** Pinhole-angular aperture spatial filtering is used to provide spatially coherent radiation.

50 to 250 eV (wavelengths from 5 to 25 nm). Further details are shown in ***Fig. 17***. The undulator is followed by a monochromator/beamline[37] that provides further monochromatization to a value of $\lambda/2\Delta\lambda = 10^3$, using a plane varied line-space grating and fixed exit slit. Various reflective optics are used to illuminate the entrance pinhole of the EUV interferometer at a 65 : 1 demagnification with a numerical aperture that approximates that of the optical system under test. Spatially and spectrally coherent EUV radiation available after pinhole and monochromator filtering is shown in ***Fig. 17B*** as a function of photon energy. Theoretically, tunable EUV radiation power of

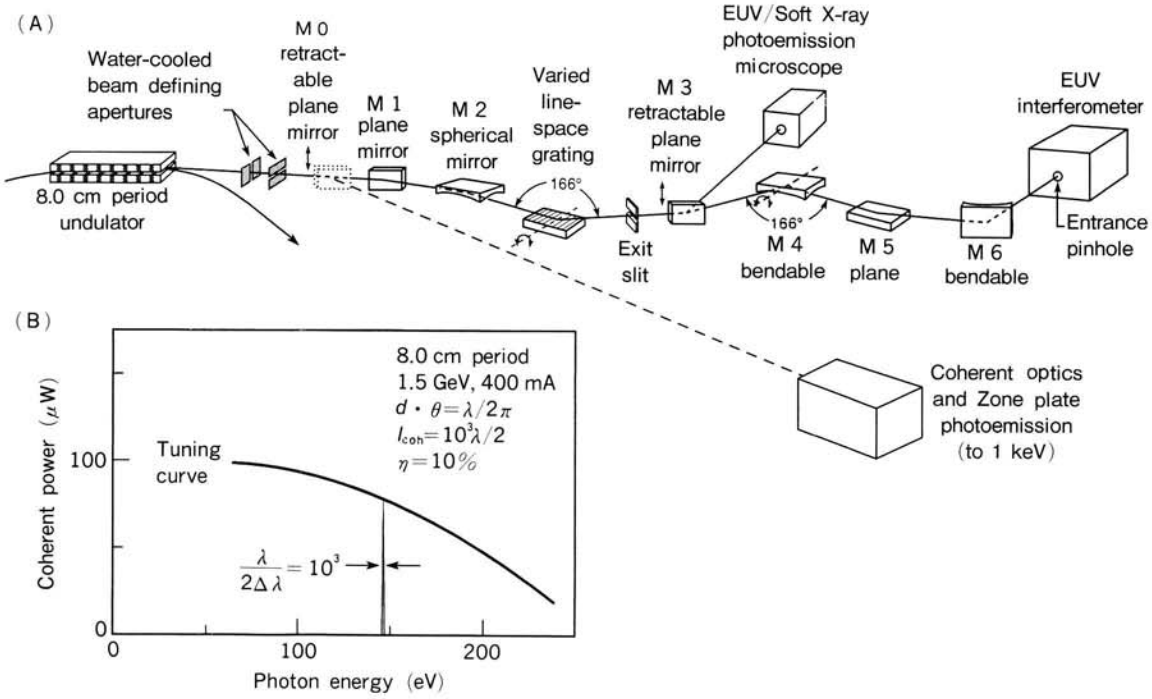

Fig. 17 **The undulator and beamline (A) used to provide spatially and spectrally coherent power at EUV wavelengths.** Average coherent power within a relative spectral bandwidth of $\lambda/2\Delta\lambda = 10^3$ is shown in (B).

order 100 μW is expected, but in practice a factor of ten less is achieved at this time, due to under-spec beamline components. These components are scheduled for replacement in the coming months. ***Figure 17A*** shows a soon to be installed branchline for EUV/soft x-ray photoemission microscopy, as well as a future expansion branchline for the study of coherent EUV and soft x-ray techniques. The latter is only in the discussion and early planning stages at this time. ***Figure 18*** shows a measured far-field pinhole-diffraction pattern, or Airy pattern, obtained at 13.4 nm wavelength on this beamline, at a position downstream of the pinhole shown at the end of the beamline in ***Fig. 17A*** (within the EUV interferometry chamber). The central portion of the central lobe is used for EUV interferometry as described in the preceding section.

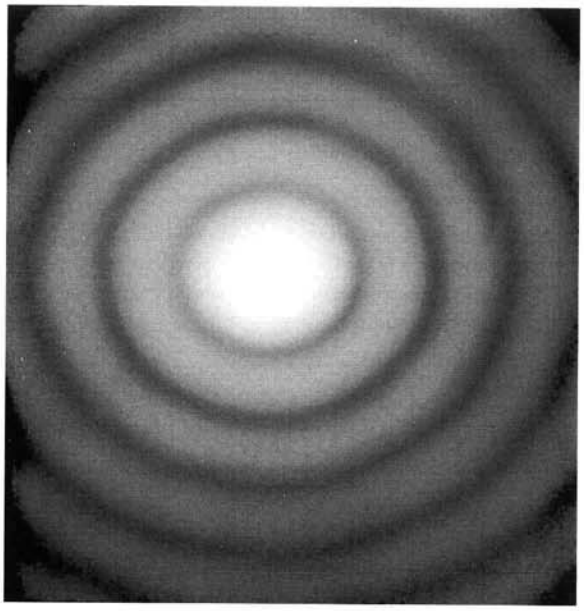

$\lambda = 13.4$ nm

Fig. 18 **Spatially coherent EUV radiation is illustrated by this Airy pattern measured at 13.4 nm wavelength to have a coherent power of about 7 μW in the central lobe.**

6. At-Wavelength Defect Inspection

Inspection of masks, or reticles, for printable defects is an important issue for all lithographies as they contain extremely complicated patterns, becoming more complex and costly to repair or replace with each succeeding generation. For EUV lithography it is anticipated that mask patterning will be accomplished through the deposition of an absorbing pattern on the surface of a flat multilayer mirror[38,39]. There is the possibility of a defect being introduced on the mask blank (the substrate) during the coating process, during application of the absorber pattern, or during subsequent handling. Substantial effort has been expended recently to reduce the introduction of defects in the coating process[40].

Several experimental efforts to characterize printable EUV defects have already been conducted. In the first measurements of this nature[41], it was shown that owing to subtle interference effects[42], sub-resolution substrate defects can impose significant wavefront phase distortion

to the reflected wave, observed as "phase defects" at the wafer. ***Figure 19*** shows the results of early experiments[41], in which programmed substrate defects (25 nm thick, gold lines, squares, and large crosses ranging in size from sub-resolution lateral widths to resolvable widths at the EUV wavelengths) were covered with a multilayer reflection coating, followed by a top layer absorber pattern, and then imaged at 14 nm wavelength with the NTT EUVL projection optics[43] at the Photon Factory. ***Figure 19A*** shows an optical phase-contrast microscope image of the mask, showing the 150 nm thick absorber lines in the foreground and the 25 nm thick programmed defects in the background. Quoted defect sizes are as measured on the mask. ***Figure 19B*** shows the 5 : 1 reduced EUV image in SAL 601 photoresist, as observed with an atomic force microscope (AFM). For example, the effect of a 2 μm square substrate defect on a 6 μm line (1.2 μm at the wafer) is evident. These early results suggest that at-wavelength EUV inspection techniques will be an important complement to existing methodologies. More recent experiments[44] suggest that coating defects, which are difficult to discern by optical or SEM techniques, are observable by high resolution at-wavelength inspection. This is now an area for active pursuit for the success of EUV lithography.

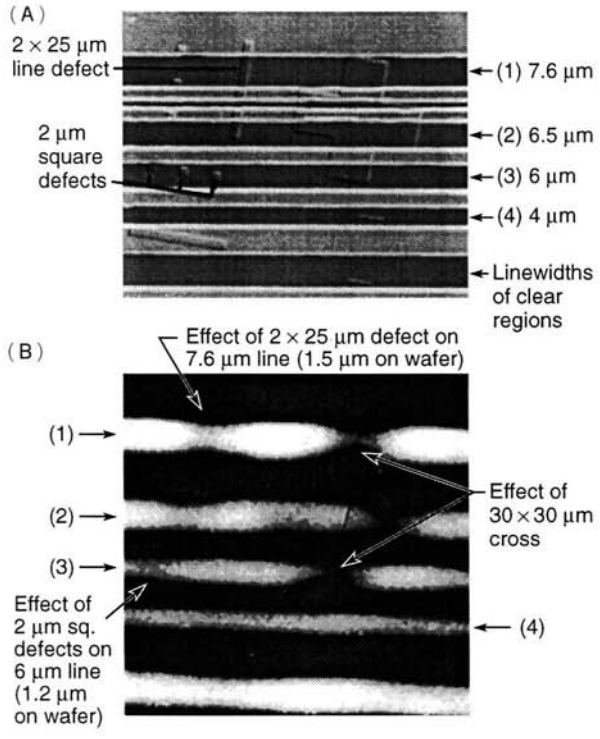

Fig. 19 **(A) Phase contrast microscope image of a portion of an EUVL mask consisting of programmed substrate defects (including a 30 μm × 30 μm cross in the upper right quadrant), coated with 30 bilayers of a Mo/Si multilayer, and a top layer gold absorber pattern of horizontal lines. (B) An EUV image of the same area recorded in SAL 601 resist and imaged by an atomic force microscope, showing the printability of various defects through the absorber pattern** (Ref. 41).

7. Conclusion

The success of extreme ultraviolet lithography for manufacturing electronic devices with critical dimensions of 0.1μm and smaller will require the development of a suite of "at-wavelength" metrologies to complement those already available. These will include high-accuracy, at-wavelength reflectometry, scattering, interferometry, and defect inspection. The development of an appropriate infrastructure is well under way in Berkeley, with very encouraging early results in all areas.

References

1) *National Technology Roadmap for Semiconductors*. (1994)
2) Bjorkholm JE, Bokor J, Eichner R, Freeman R, Gregus J, Jewell TE, Mansfield WM, MacDowell AA, Raab EL, Silfvast WT, Szeto LH, Tennant DM, Waskiewicz WK, White DL, Windt DL Wood OR II and Bruning JH : J. Vac. Sci. Technol. **B8**, 509 (1990) ; and more recently : Tichenor D, Ray-Chaudhuri A, Kubiak G, Nguyen K, Harney S, Berger K, Nissen R, Perras Y, Jin P, Weingarten L, Keifer P, Stulen R, Shagam R,Sweatt W, Smith T, Wood O, MacDowell A, Bjorkholm J, Jewell T, Zernike F, Fix B, and Hauschildt H : *Extreme Ultraviolet Lithography*, ed. by Kubiak GD and Kania DR (Optical Society of America, Washington, D.C., 1996) p. 2
3) Kinoshita H, Kurihara K, Ishii Y and Torii, Y : J. Vac. Sci. Technol. **B7**, 1648 (1989)
4) Spiller E : *Soft X-ray Optics* (SPIE. Bellingham, WA, 1994) ; Barbee T, MrowkaS and Hettrick M : Appl. Optics **24**, 883 (1985)
5) Underwood JH and Barbee RW : Nature **294**, 429 (1981) ; Underwood JH and Barbee TW : Appl. Optics **20**, 3027 (1981)
6) Henke BL, Gullikson EM, and Davis JC : Atomic Data and Nucl. Data Tables **54**, 181 (1993)
7) Windt DL, Hull R, and Waskiewicz WK : J. Appl. Phys. **71**, 2675 (1992) ; Windt DL, Waskiewicz WK and Griffith JE : Appl. Optics **33**, 2025 (1994)
8) Stearns DG : J. Appl. Phys. **71**, 4286 (1992) ; Takenaka H, Kawamura T, Ishii Y,Haga T and Kinoshita H : *Extreme Ultraviolet Lithography*, ed. by Zernike F and Attwood D (Optical Society of America, 1995) p. 26
9) Skulina KM, Alford CS, Bionta RM, Makowieki DM, Gullikson EM, Soufli R, Kortright JB and Underwood JH : Appl. Optics **34**, 3727 (1995) ; Kortright JB : J. Magnetand Magn. Mat. **156**, 271 (1996)
10) Williamson DM : *Extreme Ultraviolet Lithography* (1994)
11) Sweeney D *et al.* : private communication.
12) Bajuk D : private communication.
13) Ito M, Katagin S, Yamanashi H, Seya E, Ogawa T, Oizumi H and Terasawa T : *Extreme Ultraviolet Lithography* (1996) p. 9
14) Murakami K, Oshino T, Shimizu S, Wasa W, Kondo H, Ohtani M, Kandaka N, Mishima K and Nomura K : *ibid*. p. 16
15) Kortright JB, Gullikson EM, and Denham PE : Appl.

Optics. **32**, 6961 (1993)
16) Windt DL and Waskiewicz WK : J. Vac. Sci. Technol. **B12**(6), 3826 (1994)
17) Vernon SP, Carey MJ. Gaines DP, and Weber FJ : *Extreme Ultraviolet Lithography,* ed. by Zernike F and Attwood D (Optical Society of America, 1994) p. 33
18) Nguyen TD, Khan-Malek C, and Underwood JH : *ibid.* p. 56 ; Windt DL, Brown WL, Volkert CA and Waskiewicz WK : J. Appl. Phys. **78**, 2423 (1995)
19) Underwood JH, Gullikson EM and Nguyen K : Appl. Optics. **32**, 6985 (1993)
20) Sommargren GE : *Extreme Ultraviolet Lithography* (1996) p. 108
21) Vernon S, Gaines D, Stearns D (LLNL) and Gullikson E, Mrowka S and Underwood J (LBNL) : unpublished (1996)
22) Underwood JH, Gullikson EM, Koike M, Batson PJ, Denham PE, Franck KD, Tackaberry RE and Steele WF : Rev. Sci. Instrum. **67** (9), 1 (1996)
23) Hitachi Corporation.
24) Underwood JH and Gullikson E : unpublished.
25) Underwood JH : *Extreme Ultraviolet Lithography* (1996) p. 162
26) Stearns DG, Gaines DP, La Fontaine B, Sommargren GE, Sweeney DW, Kania DR and Ceglio NM : *Extreme Ultraviolet Lithography* (1996) p. 167 ; also Gaines DP *et al.*, p. 199 ; La Fontaine B *et al.*, p. 203
27) Gullikson E, Mrowka S, Underwood J (LBNL), and Stearns D, Gaines D and Vernon S (LLNL) : unpublished (1996)
28) Born M and Wolf E : *Principles of Optics*, sixth edition, chapters 7 and 10. (1983)
29) Hecht E : *Optics*, second edition (1987)
30) Sommargren GE : *Extreme Ultraviolet Lithography* (1996) p. 108
31) Attwood D, Sommargren G, Beguiristain R, Nguyen K, Bokor J, Ceglio N, Jackson K, Koike M and Underwood J : Appl. Optics **32**, 7022 (1993)
32) Medecki H, Tejnil E, Goldberg K, and Bokor, J : Optics Lett. **21**, 1526 (1996)
33) Tejnil E, Goldberg K, Medecki H, Beguiristain R, Bokor J and Attwood D : *Extreme Ultraviolet Lithography* (1996) p. 118
34) Attwood D. Halbach K. and Kim K-J : Science **228**, 1265 (1985)
35) Anderson E, Boegli V, and Muray L : J. Vac. Sci. Technol. **B13**(6), 2529 (1995)
36) Tejnil *et al.* : reference 33, for a description of what is described there as the "conventional" PDI.
37) Underwood J, *et al.* : unpublished. ; Beguiristain R, Underwood J, Koike M, Batson P, Medecki H, Rekawa S, Jackson K and Attwood D : Rev. Sci. Instrum. **67**(9), 1 (1996)
38) Hawryluk A, Ceglio N, and Gaines D : J. Vac. Sci. Technol. **B7**, 1702 (1989)
39) Tennant D, Bjorkholm J, D'Souza R and Eichner L : J. Vac. Sci. and Technol. **B9**, 3176 (1991)
40) Vernon S, Kania D, Kearney P. Levesque R. Hayes A, Druz B, Osten E, Rajan R and Hedge H : *Extreme Ultraviolet Lithography* (1996) p. 44
41) Nguyen K, Mizota T, Haga T, Kinoshita H and Attwood D : J. Vac. Sci. Technol. **B12**(6), 3833 (1994) ; Nguyen K : Ph.D. Thesis, Department of Electrical Engineering and Computer Science, University of California, Berkeley (1994)
42) Nguyen K, Wong A, Neureuther A, and Attwood D : *Soft X-ray Projection Lithography,* ed. by Hawryluk AM and Stulen RH (Optical Society of America, 1993) p. 47
43) Kinoshita H, Kurihara K, Mizota T and Haga T : Appl. Optics **32**, 7079 (1993)
44) Nguyen K, Mac Dowell A, Fujii K, Tennant D and Fetter L : *Extreme Ultraviolet Lithography* (1996) p.49

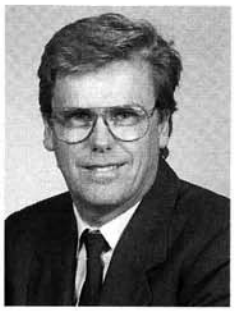

David T. ATTWOOD

David T. Attwood received an Engineering Science, Applied Physics doctorate from the New York University in 1972. From 1972 to 1983 he was a physicist at the Lawrence Livermore National Laboratory; he has been the Founding Director of the Center for X-Ray Optics, Lawrence Berkeley National Laboratory since 1983, and also has been the Professor in Residence, College of Engineering, University of California, Berkeley since 1989.

This paper is a part of the investigation perfomed under the management of FED (R&D Association for Future Electron Devices) as a part of the Industrial Science and Technology Frontier Program supported by NEDO (New Energy and Industrial Technology Development Organization)